



$$\begin{aligned} \dot{q}_{\text{use}} + \dot{q}_{\text{b}} + c_{\text{eff}} \cdot \frac{dT_f}{dt} &= h_i \cdot (T_p - T_f) \\ &= \dot{q}_{\text{abs}} - \dot{q}_{\text{sky}} - \dot{q}_{\text{conv}} - \dot{q}_{\text{cond}} \end{aligned} \quad (3)$$

with

$$\dot{q}_{\text{use}} = \dot{v} c_p \rho (T_o - T_i) \quad (4)$$

$$\dot{q}_{\text{b}} = U_b (T_f - T_a) \quad (5)$$

$$T_f = (T_o + T_i)/2 \quad (6)$$

$$\dot{q}_{\text{abs}} = K_{\alpha,b}(\theta, \gamma'_s) \cdot \alpha_{\perp} \cdot G_{\text{bT}} + K_{\alpha,d} \cdot \alpha_{\perp} \cdot G_{\text{dT}} \quad (7)$$

$$\begin{aligned} \dot{q}_{\text{sky}} &= \varepsilon_{\text{eff}} \cdot \sigma \cdot (T_p^4 - T_{\text{sky}}^4) \\ &= \varepsilon_{\text{eff}} \cdot \sigma \cdot (T_p + T_{\text{sky}}) \cdot (T_p^2 + T_{\text{sky}}^2) \cdot (T_p - T_{\text{sky}}) \\ &\approx U_R \cdot (T_p - T_{\text{sky}}) \end{aligned} \quad (8)$$

The latter assumption can be made since the term  $\sigma \cdot (T_p + T_{\text{sky}}) \cdot (T_p^2 + T_{\text{sky}}^2)$  is almost constant in the relevant temperature range.

Following a common approach, the convective heat transfer coefficients are assumed to increase linear with the wind speed.

$$\begin{aligned} \dot{q}_{\text{conv}} &= (U_{c0} + U_{c1} \cdot v_W) \cdot (T_p - T_a) \\ &= U_c \cdot (T_p - T_a) \end{aligned} \quad (9)$$

It has to be considered that the absorber surface temperature may be above as well as below the ambient temperature. To be able to distinguish between areas with convective gains and losses a ‘‘convection factor’’  $0 \leq f_{\text{conv}} \leq 1$  is introduced.  $f_{\text{conv}}$  describes the part of the absorber which is colder than the ambient temperature which leads to power gains, cf. fig. 1.

$$f_{\text{conv}} := \frac{\min[T_{p,o}; \max(T_a; T_{p,i})] - T_{p,i}}{T_{p,o} - T_{p,i}} \quad (10)$$

For the usual case  $T_a < T_{p,i}$  eq. (10) leads to  $f_{\text{conv}} = 0$ . The effective absorber temperature  $T_p^+$  of the share of the absorber surface with convective power gains can then be described by

$$T_p^+ = T_{p,i} + (T_p - T_{p,i}) \cdot f_{\text{conv}} \quad (11)$$

and analogous  $T_p^-$  for the convective losses can be determined by

$$T_p^- = T_{p,o} + (T_p - T_{p,o}) \cdot (1 - f_{\text{conv}}) \quad (12)$$

The convective heat transfer can then be modelled as

$$\dot{q}_{\text{conv}} = \dot{q}_{\text{conv}}^+ + \dot{q}_{\text{conv}}^- \quad (13)$$

with

$$\begin{aligned} \dot{q}_{\text{conv}}^+ &= U_c^+ \cdot (T_p^+ - T_a) \cdot f_{\text{conv}} \\ &= (U_{c0}^+ + U_{c1}^+ \cdot v_W) \cdot f_{\text{conv}} \\ &\quad [T_{p,i} + (T_p - T_{p,i}) \cdot f_{\text{conv}} - T_a] \end{aligned} \quad (14)$$

$$\begin{aligned} \dot{q}_{\text{conv}}^- &= U_c^- \cdot (T_p^- - T_a) \cdot (1 - f_{\text{conv}}) \\ &= (U_{c0}^- + U_{c1}^- \cdot v_W) \cdot (1 - f_{\text{conv}}) \\ &\quad [T_{p,o} + (T_p - T_{p,o}) \cdot (1 - f_{\text{conv}}) - T_a] \end{aligned} \quad (15)$$

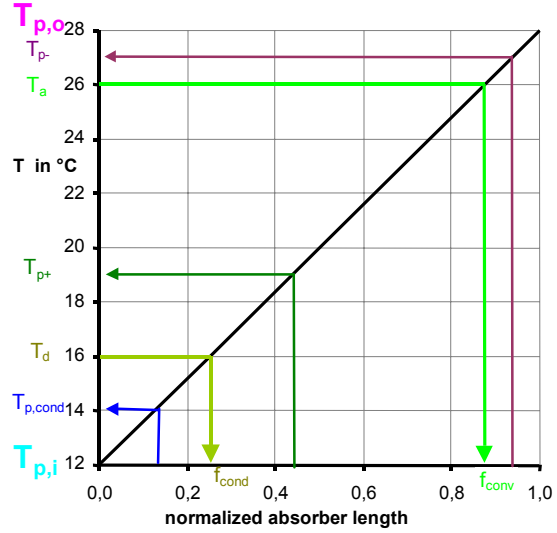


Fig. 1: Depending on the boundary conditions, three different heat transfer mechanism can take place on different areas of the absorber between fluid inlet ( $T_{p,i}$ ) and outlet ( $T_{p,o}$ ). 1.) in the absorber area with a surface temperature  $T_p$  beneath the dew point temperature  $T_d$  ( $0$  to  $f_{\text{cond}}$ ) due to condensing air humidity, 2.) for  $T_p < T_a$  ( $0$  to  $f_{\text{conv}}$ ) convective heat gains and 3.) for  $T_a < T_p$  ( $1 - f_{\text{conv}}$  to  $1$ ) convective heat losses. Effective, average absorber temperatures for the single heat transfer mechanism can be determined with the assumption of a linear increase of the surface temperature in fluid flow direction.

Following (Soltau 1989), the condensation heat flux can be determined by

$$\dot{q}_{\text{cond}} = f \cdot [p_s(T_p) - p_s(T_d)] \quad (16)$$

where  $f$  is a function of the mass transfer coefficient and of the specific evaporation enthalpy. Following (Baehr 1993), the temperature-dependent saturated vapour pressure of water can be described by:

$$p_s(T) = 10^2 \cdot \exp\left(19,016 - \frac{4064,95}{T/^\circ\text{C} + 236,25}\right) \text{ Pa} \quad (17)$$

The problem is now to linearize the partial pressure differences in eq. (17) and to convert these into

temperature differences, conforming to the model. For this purpose, the approach was made of building a matrix of coefficients containing the linearized slopes  $S$  of the vapour pressure curve for different  $T_{p,i}$  and  $\Delta T = \max[T_{p,i}; \min(T_d; T_{p,o})] - T_{p,i}$ .

After the introduction of a condensation factor and an average absorber surface temperature for the condensation heat transfer, similar to eqs. (10) and (11) for the convection,

$$f_{\text{cond}} := \frac{\min[T_{p,o}; \max(T_d; T_{p,i})] - T_{p,i}}{T_{p,o} - T_{p,i}} \quad (18)$$

$$T_{p,\text{cond}} = T_{p,i} + (T_p - T_{p,i}) \cdot f_{\text{cond}} \quad (19)$$

and with the assumption of nearly constant water vapour characteristics in the considered temperature interval, eq. (16) passes into

$$\dot{q}_{\text{cond}} = U_D \cdot S \cdot (T_{p,\text{cond}} - T_d) \cdot f_{\text{cond}} \quad (20)$$

$U_D$  can be determined by parameter fits. Under certain assumptions, cf. (Krämer 1999),  $U_D$  can be coupled with the convective heat transfer coefficient  $U_c$  (Krämer 1999):

$$U_D = 1,78 \cdot 10^{-2} \frac{K}{Pa} \cdot U_c^+ \quad (21)$$

With the latter procedure one parameter less has to be determined with the model.

Substituting eqs. (5, 8, 14, 15, 20) in eq. (3) leads to

$$\begin{aligned} \dot{q}_{\text{use}} + U_b \cdot (T_f - T_a) + c_{\text{eff}} \cdot \frac{dT_f}{dt} \\ = h_i \cdot (T_p - T_f) \\ = \dot{q}_{\text{abs}} - U_R \cdot (T_p - T_{\text{sky}}) \\ - U_c^+ \cdot (T_p^+ - T_a) \cdot f_{\text{conv}} \\ - U_c^- \cdot (T_p^- - T_a) \cdot (1 - f_{\text{conv}}) \\ - U_D \cdot S \cdot (T_{p,\text{cond}} - T_d) \cdot f_{\text{cond}} \end{aligned} \quad (22)$$

By adding temperature differences in a suitable way the right hand part of eq. (22) can be transformed into

$$\begin{aligned} h_i \cdot (T_p - T_f) = \dot{q}_{\text{abs}} \\ - U_R \cdot [(T_p - T_f) + (T_f - T_{\text{sky}})] \\ - U_c^+ \cdot [(T_p - T_f) + (T_f^+ - T_a)] \cdot f_{\text{conv}} \\ - U_c^- \cdot [(T_p - T_f) + (T_f^- - T_a)] \cdot (1 - f_{\text{conv}}) \\ - U_D \cdot S \cdot [(T_p - T_f) + (T_{f,\text{cond}} - T_d)] \cdot f_{\text{cond}} \end{aligned} \quad (23)$$

which can be solved to  $T_p - T_f$  and substituted in eq. (22). Applying eq. (9) finally leads to

$$\dot{q}_{\text{use}} + U_b (T_f - T_a) + c_{\text{eff}} \frac{dT_f}{dt} = F^* \cdot \left\{ \begin{array}{l} K_{\alpha,b}(\theta, \gamma'_s) \alpha_{\perp} G_{b,T} + K_{\alpha,d} \alpha_{\perp} G_{d,T} \\ - \varepsilon_{\text{eff}} \cdot U_R \cdot (T_f - T_{\text{sky}}) \\ - (U_{c0}^+ + U_{c1}^+ \cdot v_w) \cdot f_{\text{conv}} \\ [T_i + (T_f - T_i) \cdot f_{\text{conv}} - T_a] \\ - (U_{c0}^- + U_{c1}^- \cdot v_w) \cdot (1 - f_{\text{conv}}) \\ [T_o + (T_f - T_o) \cdot (1 - f_{\text{conv}}) - T_a] \\ - U_D S [T_i + (T_f - T_i) \cdot f_{\text{cond}} - T_d] f_{\text{cond}} \end{array} \right. \quad (24)$$

with

$$F^* = \frac{h_i}{h_i + U_R + U_c^+ f_{\text{conv}} + U_c^- (1 - f_{\text{conv}}) + U_D S f_{\text{cond}}}$$

$F^*$  is equivalent to the well known collector efficiency factor  $F'$ . However, regarding uncovered collectors the back side heat losses are related to the fluid instead of the surface temperature, cf. eq. (3).

As a result, eq. (24) contains the measuring quantities  $\dot{q}_{\text{use}}, T_f, T_a, G_{b,T}, G_{d,T}, T_{\text{sky}}, v_w, T_i, T_o$  and  $T_d$ , furthermore quantities which can be derived by the measured data, material properties or constants like  $dT_f/dt, U_R, f_{\text{conv}}, f_{\text{cond}}, S$  and furthermore the collector model parameters as  $F^* K_{\alpha,b}(\theta, \gamma'_s), \alpha_{\perp},$

$F^* K_{\alpha,d}, F^* U_R, F^* U_D, F^* U_{c0}^+, F^* U_{c1}^+, F^* U_{c0}^-, F^* U_{c1}^-$ ,  $h_i, U_b$  and  $c_{\text{eff}}$ . Some of the parameters can be determined theoretically (e.g. the  $K_{\alpha}$ 's) whereas the heat transfer coefficients have to be found out by experiments with multi linear regressions of the measured time series (Perers 1993). In principle, eq. (24) would have to be solved iteratively, because  $f_{\text{conv}}, f_{\text{cond}}$  and  $S$  can only be determined by evaluating the useful power gain

$$T_{p,*} = T_{f,*} + \frac{\dot{q}_{\text{use}}}{h_i} \quad (25)$$

which is unknown. Furthermore, the time dependency of the fluid temperature would have to be known for the consideration of the effective heat capacity. However, investigations showed that a determination of the absorber surface temperatures with measured values of  $\dot{q}_{\text{use}}$  in eq. (25) delivers de facto the same parameter values, compared to an iterative application of eq. (24) and (25).

However, if eq. (24) shall be applied for a prediction of solar energy yields, for  $f_{\text{conv}} < 1$  or  $f_{\text{cond}} > 0$  an iterative evaluation of  $\dot{q}_{\text{use}}$  is necessary.

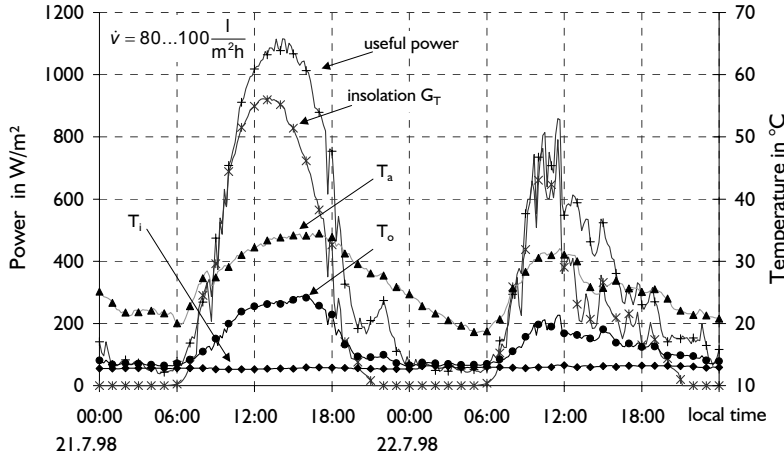


Fig. 2: Exemplary temperature courses and power measured at the uncovered collector. During those days the collector was driven with relatively high specific flow rates, thus the collector outlet temperature remained below the ambient temperature.

### 3. MEASUREMENTS

In Bishkek (Kyrgyzstan) measurements were carried out for a period of two months. Data have been recorded as one minute average values of the hemispherical-, diffuse- and long wave irradiance, flow-, return- and ambient temperature, absorber flow rate, air humidity and wind speed.

The absorber inlet temperature was between 12° and 13°C, the ambient temperatures in the range of 20° to 35°C. Thus, in most cases the ambient temperature even exceeded the collector outlet temperature. Sometimes the dew point temperature was above the fluid inlet temperature which led to condensation of air humidity at least on a part of the collector.

The average difference between average fluid and ambient temperature was nearly -9 K which led to collector efficiencies, only defined with respect to the incoming irradiance, of higher than one, cf. fig. 2.

### 4. COMPARISON TO MEASURED DATA

In the evaluation of the experiments two small neglects are included. Firstly, the thermal gains of the flow- and return pipes as well as the distribution and collecting pipes of the collector have not been taken into consideration. An estimation delivered a value of maximal 10 W/m² for these effects. Secondly, as the distributing and collecting pipes of the absorber were installed beside each other, a reduction of the aperture area due to the turn loops of the absorber strips appeared. On the other hand, the collector aperture area was complemented by additional bridges between the absorber webs. Both reversal effects are nearly in the same order of a few percent of the collector aperture area.

(Hilmer 1996) derived a two axis incident angle modifier function  $K_{\alpha,b}(\theta, \gamma'_s)$  numerically as well as  $K_{\alpha,d}$  for an absorber which was geometrically nearly identical. These functions were used for the determination of  $\dot{q}_{abs}$  in eq. (24).

The determination of all remaining parameters in eq. (24), which are  $\alpha_{\perp}$ ,  $h_i$ ,  $U_{c0}^+$ ,  $U_{c1}^+$ ,  $U_{c0}^-$ ,  $U_{c1}^-$ ,  $U_b$ ,  $\epsilon_{eff}$  and  $c_{eff}$ , by multi linear regression with the entire data set of nearly 7500 10-minute mean values failed.

For  $U_b$  ( $< 0$ ) as well as for  $\alpha_{\perp}$  and  $\epsilon_{eff}$  (both values  $> 1$ ) no physical sensible values could be determined. Also  $h_i$  was overestimated significantly. Thus, the model equation (24) has to be further restricted.

During the measured period, convective heat losses could be observed only at quite a few data sets with very low specific flow rates ( $\dot{v} \leq 20$  l/m²h). Under these conditions the model assumption of a linearly increasing fluid temperature in the absorber is not valid any more. Thus, only data sequences with flow rates between 40 and 120 l/m²h and hereby without convective losses (always  $f_{conv}=1$ ) have been taken into account in the following evaluations.

The back side of the absorber is in thermal contact with the bearing area. The roof, however, consisted of a complicated construction made of asphaltic felt, concrete and wood. Hereby it was not possible to determine a representative roof temperature for the heat exchange with the absorber. Furthermore, beneath parts of the absorber frequently condensate could be observed. A mathematical modelling of condensation and evaporation processes between roof and absorber appear to be difficult. The back side of the absorber was assumed to be adiabatic with  $U_b=0$ .

The heat transfer coefficient  $h_i$  from the absorber surface to the fluid is dominated by heat conduction in the absorber material and was numerically determined by (Schmidt 1999) with the use of the CFD-program Fluent. For laminar flow a value of  $h_i = 200$  W/m²K was found, for turbulent flow  $h_i = 290$  W/m²K, both values with respect to the collector aperture area. Sensitivity analysis showed that the value of  $h_i$  has only small influence on the other collector parameters determined.

A renewed parameter fit with the remaining parameters  $\alpha_{\perp}$ ,  $U_{c0}^+$ ,  $U_{c1}^+$ ,  $\epsilon_{eff}$  und  $c_{eff}$  resulted in mostly sensible values, only  $\alpha_{\perp} = 1.01$  was out of the ordinary. Probably a net heat flux to the absorber takes place from

the roof covering, as mentioned made of black asphaltic felt. For the effective emission coefficient of the absorber a weak minimum for  $\varepsilon_{\text{eff}}=0.73$  could be determined. A data analysis showed that the values of  $\alpha_{\perp}$  and  $\varepsilon_{\text{eff}}$  are strongly correlated. Surprisingly,  $\varepsilon_{\text{eff}}$  is no sensitive parameter for the overall result. A proper explanation might be that the sky temperature  $T_{\text{sky}}$  very often was between the absorber surface temperatures at the fluid inlet and outlet, thus the net heat exchange between absorber and sky by infrared radiation was only poor.

The effective heat capacity  $c_{\text{eff}}$  was determined about twice as high as theoretically expected. Due to the stable weather conditions during the experiments variations of  $c_{\text{eff}}$  have nearly no influence on the overall result as well.

$U_{c0}^+$  and  $U_{c1}^+$  were determined to be  $2.8 \text{ W/m}^2\text{K}$  and  $7.0 \text{ (W/m}^2\text{K)/(m/s)}$ , respectively, which is in the expected range. However, also these parameters are highly correlated. During the measurements only seldom higher wind speed was observed, furthermore the used anemometer had a starting velocity of about  $1 \text{ m/s}$ .

Energetically, the condensation did not make a big difference. If  $U_D$  remains in the model as a free parameter, cf. eq. (24), the share of  $q_{\text{cond}}$  on  $q_{\text{use}}$  was in the range of 2 %. If  $U_D$  is coupled with  $U_{c0}^+$ , eq. (21), the share of  $q_{\text{cond}}$  is about 1 %. In the latter case the condensation heat transfer coefficient is almost entirely dominated by the convective heat transfer coefficient which is about forty times more relevant regarding  $q_{\text{use}}$ . In the framework of the evaluated experiments it could not be determined which approach should be preferred. However, obviously  $q_{\text{cond}}$  was strongly overestimated if

$U_c^+$  in eq. (21) was substituted not only by  $U_{c0}^+$ , but also by the wind speed proportional coefficient  $U_{c1}^+ \cdot v_w$ .

The developed model is able to reproduce the measured collector gains for clear and for cloudy periods very well, the differences between measured and modelled power gains are nearly always within the interval of measurement precision, cf. fig. 3. For typical collector gains of 6 to  $12 \text{ kWh/m}^2\text{d}$ , the average deviation of the daily sums of the collector gains are below 5%, for the entire period below 1%.

The restrictions mentioned above regarding not determinable parameters do not make the model approach uncertain, but are caused by the specific and hardly influenced boundary conditions during the in-situ measurements.

## 5. SUMMARY

A model was developed to describe the thermal behaviour of uncovered collectors. The model covers different heat transfer coefficients of convection and condensation which can lead to heat gains and losses on different sections of the absorber surface. Thus, the shares of the single quantities of heat contributed by different heat transfer paths can be determined. Main model assumption is a linear increase of the absorber surface temperature in direction of the fluid flow, thus the application is limited to sufficiently high flow rates.

The results of the model have been compared with data measured at an uncovered collector of  $50 \text{ m}^2$  for two months. However, due to very low fluid inlet temperatures and high ambient temperatures convective heat losses of the absorber have been observed only seldom and the model could not have been validated complete yet.

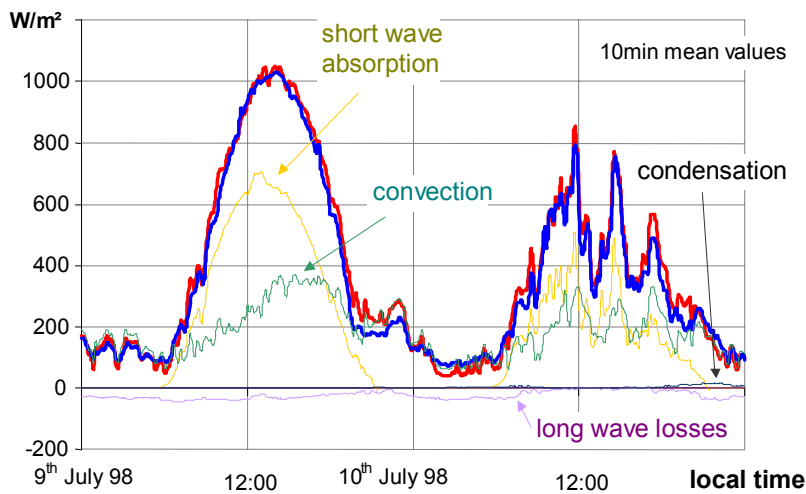


Fig. 3: Comparison of the measured (blue) and modelled (red) collector power gain for two typical measured days. Following the determined parameter and the single terms in eq. (24), the cumulative heat gains due to absorption of solar irradiance have been only 20% higher compared to the convective heat gains.

## NOMENCLATURE

All area specific quantities are related to the aperture area of the collector.

$c_{\text{eff}}$	$\text{J/m}^2\text{K}$	effective heat capacity of the collector	$T_f$	$^{\circ}\text{C}$	average fluid temperature = $(T_i+T_o)/2$
$c_1 \dots c_6$	different	constants in the model equation of EN 12795 (2001)	$T_i$	$^{\circ}\text{C}$	inlet temperature of the absorber
$E_L$	$\text{W/m}^2$	long wave irradiance	$T_o$	$^{\circ}\text{C}$	outlet temperature of the absorber
$f_{\text{cond}}$	-	share of the collector aperture area where condensation takes place	$T_p$	$^{\circ}\text{C}$	average absorber surface temperature = $(T_{p,i}+T_{p,o})/2$
$f_{\text{conv}}$	-	share of the collector aperture area where convective heat gains take place	$T_{p,i}$	$^{\circ}\text{C}$	absorber surface temperature at the fluid inlet
$F^*$	-	uncovered collector efficiency factor	$T_{p,o}$	$^{\circ}\text{C}$	absorber surface temperature at the fluid outlet
$F'$	-	collector efficiency factor	$T_p^+$	$^{\circ}\text{C}$	average temperature of the share of the absorber surface with convective heat gains
$G_T$	$\text{W/m}^2$	hemispherical radiation in the collector plane	$T_p^-$	$^{\circ}\text{C}$	average temperature of the share of the absorber surface with convective heat losses
$G_{bT}$	$\text{W/m}^2$	hemispherical beam radiation in the collector plane	$T_{p,\text{cond}}$	$^{\circ}\text{C}$	average temperature of the share of the absorber surface where condensation takes place
$G_{dT}$	$\text{W/m}^2$	hemispherical diffuse radiation in the collector plane	$T_{\text{sky}}$	K	sky temperature, equivalent to the black body radiation from the sky
$h_i$	$\text{W/m}^2\text{K}$	heat transfer coefficient between collector surface and fluid	$U_b$	$\text{W/m}^2\text{K}$	heat transfer coefficient on the back side of the absorber
$K_{\alpha,b}$	-	incident angle modifier function for beam radiation	$U_D$	$\text{W/m}^2\text{K}$	condensation heat transfer coefficient
$K_{\alpha,d}$	-	incident angle modifier constant for diffuse radiation	$U_c$	$\text{W/m}^2\text{K}$	convection heat transfer coefficient
$p_s$	Pa	saturated vapour pressure of water	$U_{c0}$	$\text{W/m}^2\text{K}$	wind independent part of the convection heat transfer coefficient
$\dot{q}_{\text{abs}}$	$\text{W/m}^2$	heat flux by short wave radiation	$U_{c1}$	$\text{Ws/m}^3\text{K}$	wind dependent part of the convection heat transfer coefficient
$\dot{q}_b$	$\text{W/m}^2$	back side heat flux from or to the absorber	$U_c^+$	$\text{W/m}^2\text{K}$	heat transfer coefficient for convective gains
$\dot{q}_{\text{conv}}$	$\text{W/m}^2$	convective heat flux	$U_c^-$	$\text{W/m}^2\text{K}$	heat transfer coefficient for convective losses
$\dot{q}_{\text{conv}}^+$	$\text{W/m}^2$	convective power gains	$U_R$	$\text{W/m}^2\text{K}$	heat transfer coefficient for long wave radiation
$\dot{q}_{\text{conv}}^-$	$\text{W/m}^2$	convective power losses	$U'_R$	$\text{W/m}^2\text{K}$	$:= U_R / \varepsilon_{\text{eff}}$
$\dot{q}_{\text{cond}}$	$\text{W/m}^2$	heat flux by condensation	$v_w$	m/s	wind speed in the collector plane
$q_{\text{cond}}$	$\text{W/m}^2$	heat gain by condensation	$\dot{v}$	$\text{l/m}^2\text{h}$	specific flow rate
$\dot{q}_{\text{sky}}$	$\text{W/m}^2$	heat flux by long wave radiation	$\alpha_{\perp}$	-	absorption coefficient at normal incident
$\dot{q}_{\text{use}}$	$\text{W/m}^2$	useful power gain	$\varepsilon_{\text{eff}}$	-	effective emission coefficient of the absorber surface
$q_{\text{use}}$	$\text{Wh/m}^2$	useful energy gain	$\gamma'_s, \theta$	$^{\circ}$	incident angles of the beam radiation
$S$	$\text{K/Pa}$	approximated slope of the linearized saturated vapour pressure curve	$\rho$	$\text{kg/m}^3$	density
$T_a$	$^{\circ}\text{C}$	ambient temperature	$\sigma$	$\text{W/m}^2\text{K}^4$	Stefan-Boltzmann constant
$T_d$	$^{\circ}\text{C}$	dew point temperature			

## LITERATURE

- Baehr, H.D. (1993): Thermodynamik, *Springer Verlag* Berlin, 8. Auflage
- Hilmer, F. (1996): Modellierung des Betriebsverhaltens nicht abgedeckter Sonnenkollektoren bei zeitlich veränderlichem Fluidstrom, *Dissertation*, Universität Marburg
- ISO 9806-3 (1995): Test Methods for Solar Collectors – Part 3: Thermal Performance of Unglazed Liquid Heating Collectors (Sensible Heat Transfer only) Including Pressure Drop
- Krämer, M. (1999) Untersuchung des Einsatzes ungedeckter Kollektoren zur Vorerwärmung von Frischwasser im Fernwärmenetz Bischkek (Kirgisien), *Diplomarbeit*, Universität Marburg, FB Physik
- Perers, B. (1987): Performance Testing of Unglazed Collectors, *Report for IEA Task III*, Studsvik Energy, Sweden
- Perers, B. (1993) Dynamic Method for Solar Collector Array Testing and Evaluation with Standard Database and Simulation Programs, *Solar Energy* **50**, 6, pp. 517-526
- EN 12975-2 (2001), Thermal Solar Systems - Collectors - Part 2: Test methods
- Schmidt, R. (1999): personal talk, Braunschweig Technical University
- Soltau, H. (1989): Das thermische Verhalten offener Kollektoren, *VDI-Verlag* Düsseldorf
- Vajen, K., Krämer, M., Orths, R., Boronbaev, E.K. (1999) Solar Absorber System for Preheating Feeding Water for District Heating Nets, *Proc. ISES Solar World Congress*, 4.-9.7.1999, Jerusalem, Vol III, pp. 90-91

## ACKNOWLEDGEMENTS

The authors like to thank especially the following institutions for financial and logistical support: International office of the BMBF, Wagner&Co Solartechnik Lmt. in Cölbe (Germany), Heat and Power Plant of Bishkek City (Kyrgyzstan). R. Schmidt (Technische Universität Braunschweig, Germany) carried out CFD calculations.